Preprint ANL/MCS-P1693-1109

COMPUTING $f(A)b$ VIA LEAST SQUARES POLYNOMIAL APPROXIMATIONS

JIE CHEN*, MIHAI ANITESCU†, AND YOUSEF SAAD*

Abstract. Given a certain function f, various methods have been proposed in the past for addressing the important problem of computing the the matrix-vector product $f(A)b$ without explicitly computing the matrix $f(A)$. Such methods were typically used to compute a specific function f, a common case being that of the exponential. This paper discusses a procedure based on least squares polynomials that can, in principle, be applied to any (continuous) function f. The idea is to start by approximating the function by a spline of a desired accuracy. Then, a particular definition of the function inner product is invoked that facilitates the computation of the least squares polynomial to this spline function. Since the function is approximated by a polynomial, the matrix A is referenced only through a matrix-vector multiplication. In addition, the choice of the inner product makes it possible to avoid numerical integration. As an important application, we consider the case when $f(t) = \sqrt{t}$ and A is a sparse, symmetric positive-definite matrix, which arises in sampling from a Gaussian process distribution. The covariance matrix of the distribution is defined by using a covariance function that has a compact support, at a very large number of sites that are on a regular or irregular grid. We derive error bounds and show extensive numerical results to illustrate the effectiveness of the proposed technique.

Key words. Matrix function, Least squares polynomials, Gaussian process, sampling

AMS subject classifications. 65F35, 65F30, 65F50

1. Introduction.

It is often necessary to compute a matrix-vector product $f(A)b$, where f is a matrix function defined on the spectrum of A and b is a column vector. Examples of such functions f include the exponential $\exp(A)$, the logarithm $\log(A)$, and the square root $A^{1/2}$. In the common situation when A is symmetric real (or Hermitian), then $A = VDV^T$, where D is the diagonal matrix consisting of real eigenvalues and V is the orthonormal matrix of corresponding eigenvectors. Then, by definition, the matrix function $f(A)$ can be rewritten as $f(A) = Vf(D)V^T$, where f in effect acts on the diagonal of D elementwise. When A is large, its diagonalization may not be practically feasible. Even when A is small, its diagonalization may not be numerically viable in the nonsymmetric case, and the above approach will not be safe. This is illustrated in the well-known papers [21, 22] for the exponential function and, more generally, in the recent treatise [16].

In this paper we address the case when A is a large sparse matrix and f is any continuous function. We restrict our study to the case where A is symmetric real (or Hermitian complex), although the proposed approach can also be applied to the case, rare in practice, when A is nonsymmetric and has real eigenvalues. This situation precludes a full-fledged diagonalization of A. A preferred approach advocated in the literature is to exploit the nature of the problem: since we need to compute the product of $f(A)$ by b, there is no need to compute $f(A)$. The situation is similar to that of solving linear systems which corresponds to the case when $f(t) = 1/t$. In

*Department of Computer Science and Engineering, University of Minnesota at Twin Cities, Minneapolis, MN 55455. Email: {jchen,saad}@cs.umn.edu. Work of these authors was supported by NSF grant DMS-0810938 and by DOE grant DE-FG-08ER25841.

†Mathematics and Computer Science Division, Argonne National Laboratory, Argonne, IL 60439. Email: anitescu@mcs.anl.gov. Work of this author was supported by the U.S. Department of Energy, through Contract No. DE-AC02-06CH11357.

such situations there is no need to invert A, and inexpensive methods (e.g., based on Krylov subspaces) can be designed to solve the problem.

The case $f(A) = \exp(A)$ was extensively studied (see, e.g., [28, 13, 17, 18, 3]). Some approaches have also been considered in the literature for a general function f, most notably with the use of Krylov subspace methods (see, e.g., [34, 35]). In these methods, an Arnoldi process (a Lanczos process in the symmetric case) with an initial vector $b/\left\|b\right\|_2$ yields in k steps a matrix Q_k with k orthonormal columns and a $k \times k$ Hessenberg matrix H_k (tridiagonal in the symmetric case). Then, $f_k = \left\|b\right\|_2 Q_k f(H_k) e_1$ is a progressive approximation to $f(A)b$ as k increases. It remains to compute $f(H_k)e_1$, which is usually much easier than the original problem because k is typically small. (We note the related problem of computing the quadratic form $b^T f(A)b$, see, e.g., [2, 14].) Thus, [2] uses a similar idea, essentially performing an approximate eigen-decomposition of the symmetric positive definite A using the Lanczos process. The product $b^T f(A)b$ is written in a Riemann-Stieltjes integral form, and because of the orthogonality of the Lanczos vectors (or the associated polynomials), the Lanczos procedure applied to this problem will yield an approximation that can be viewed as an estimate of the integral via a quadrature rule.

Other methods have also been proposed in the literature; for a comprehensive treatise, see [16]. In integral/ODE methods [6, 1], some common functions f are known to be an integral of some other function g or the solution to a differential equation. In these cases, numerical integration techniques can be adapted to compute $f(A)b$. In some cases, however, the integration may be inefficient unless A is not too ill conditioned. Recently, Saad [29] proposed a conjugate residual-type method for approximating $f(A)b$, addressing mostly the case when f is an approximate step function. The method can be viewed as a modification of the traditional conjugate residual method for solving linear systems to compute an optimal residual polynomial. It can be adapted to any function f with a finite value at the origin. For a brief discussion of this approach, see Section 6.4.

We consider approximating f by a least squares polynomial, based on an idea originating from an unpublished technical report [10]. Various forms of polynomial approximation approaches [9, 23, 24] have been exploited to approximate $f(A)b$ by $p(A)b$, where p denotes a polynomial. A common approach is to expand f in a basis of orthogonal polynomials, such as Chebyshev, (see, e.g., [3, 9]). Since these expansions are not explicitly known for an arbitrary function, the approach is limited to very specific functions, for example, the exponential. There have been extensions of this basic idea, specifically for the nonsymmetric case, by exploiting asymptotically optimal approximations, using, for example, Faber polynomials or Fejer polynomials, (see, e.g., [23, 24]). There are advantages and disadvantages to these approaches when compared with Krylov methods. Krylov methods are general purpose and require no estimates of eigenvalues. In contrast, methods based on approximation theory usually require determining a set in the real or complex space that contains the spectrum of A. On the other hand, approximation theory methods tend to be effective for certain functions [3] and they are often easier to analyze theoretically.

The method proposed in this paper computes an approximation to $f(A)b$ by determining the polynomial ϕ_{k+1} that is close to f with respect to some weighted L_2 norm. Determining the least squares polynomial approximation to f would normally entail computing expansion coefficients that require numerical integration. To avoid this, we first approximate f by a spline function s, which is approximated, in place of f, by the polynomial ϕ_{k+1}. Then, the expansion coefficients are easy to extract without

numerical quadrature, provided appropriate weights of the spline approximation are used in each interval.

This paper was initially motivated by a statistical sampling problem (see Section 5.1), that leads to a situation where $f(t) = \sqrt{t}$ and A is symmetric positive (semi)-definite. It turns out that a simple technique, possibly one of the best approaches in this case, is to expand f in Legendre polynomials. The coefficients are then known explicitly; see, for example, [20, p. 59]. Here, we do not consider the Legendre polynomials approach because we want to emphasize *generality*. The method we propose is applicable to any function, not only those that happen to have a known expansion in some orthogonal basis of polynomials. Indeed, the only requirement for our technique to work well is that the function f be well approximated by a spline.

Error bounds will be established for the proposed method, which suggest that functions that are not differentiable or have large derivatives in the interval will be difficult to approximate by polynomials. This is the case for $f(t) = \sqrt{t}$, which causes difficulties near the origin. Experimental tests demonstrate the capability of the proposed method for this case for large-scale problems. Numerical results indicate promising performance when this problem goes to extreme scales. We also show experimental results for other functions, such as the logarithm and the exponential, demonstrating the wide applicability of the proposed method.

2. Approximating $f(A)b$. A conceptual framework for computing the matrix-vector product $f(A)b$ is to approximate the function f by a polynomial. Assume that $\Lambda(A)$, the spectrum of A, is included in some interval $[l, u]$ and that f is defined and continuous on $[l, u]$. Then, f can be approximated to arbitrary accuracy by a polynomial. In particular, we can readily compute an approximation that is optimal, in the least squares sense, over any polynomial subspace. If an orthonormal basis $\{P_j(t) \mid j = 1, 2, \ldots, k+1\}$ for the polynomial space is given, then this optimal approximation is

$$f(t) \approx \sum_{j=1}^{k+1} \gamma_j P_j(t), \quad \text{with} \quad \gamma_j = \langle f(t), P_j(t) \rangle ,$$

where $\langle g, h \rangle$ represents the function inner product between g and h associated with a weight w:

$$\langle g, h \rangle = \int_l^u g(t)h(t)w(t)\, dt. \tag{2.1}$$

We will defer the discussion of the choice of the weight function w to the next section. Here, we simply note that, with a proper choice, numerical integration (e.g., by quadrature) can be avoided. The norm of a function g is correspondingly defined as the induced norm from the inner product:

$$\|g(t)\| := \langle g(t), g(t) \rangle^{1/2} . \tag{2.2}$$

The Stieltjes procedure generates the required basis. Let $\mathbf{1}$ denote the constant function with value 1. With the initial condition $P_0(t) = 0$ and $P_1(t) = \mathbf{1}/\|\mathbf{1}\|$, the Stieltjes procedure computes a sequence of polynomials $P_j(t)$ with the help of a three-term recurrence of the form

$$\beta_{j+1} P_{j+1}(t) = tP_j(t) - \alpha_j P_j(t) - \beta_j P_{j-1}(t), \qquad j = 1, \ldots, k, \tag{2.3}$$

where α_j is the inner product between $tP_j(t)$ and $P_j(t)$ and where β_{j+1} is a normalization coefficient that ensures that $P_{j+1}(t)$, a polynomial of degree j, has unit norm. The resulting polynomials $\{P_j(t)\}$ form an orthonormal basis of the space $\mathbb{P}_{k+1}$ of all polynomials of degree not exceeding k.

Define v_j to be $P_j(A)b$. If $\Lambda(A) \subset [l, u]$, we can approximate $f(A)b$ as follows:

$$f(A)b \approx \sum_{j=1}^{k+1} \gamma_j P_j(A)b \;=\; \sum_{j=1}^{k+1} \gamma_j v_j. \tag{2.4}$$

Relation (2.3) induces the following three-term recurrence relation for the v_j's:

$$\beta_{j+1} v_{j+1} = Av_j - \alpha_j v_j - \beta_j v_{j-1}. \tag{2.5}$$

Formula (2.5) resembles the three-term recurrence of the Lanczos process for generating an orthonormal basis of a Krylov subspace related to a symmetric matrix A. This resemblance is not surprising because the Lanczos algorithm is nothing but a Stieljes procedure for computing orthogonal polynomials with respect to a discrete inner product over the space of polynomials [14]. In this paper a continuous inner product is used in the Stieljes procedure; see the next section.

Algorithm 1 shows a detailed procedure for approximating $f(A)b$ via a sequence of vectors $z_j := \sum_{j'=1}^{j} \gamma_{j'} v_{j'}$ based on relations (2.4) and (2.5). The initial basis polynomial $P_1(t)$ is computed in line 2, and the initial vectors v_0 and v_1 are computed in line 3. Then, the first approximant z_1 is computed in lines 4 and 5. In the loop, lines 7 to 10 compute a new basis polynomial $P_{j+1}(t)$ via the three term recurrence, and line 11 computes the corresponding vector v_{j+1}. Then, lines 12 and 13 update the approximant z_j; and, after k steps, the algorithm returns the vector z_{k+1}.

Algorithm 1 Approximating $f(A)b$, initial version

1: $P_0(t) = 0$
2: $S_0(t) = 1$, $\beta_1 = \|S_0(t)\|$, $P_1(t) = S_0(t)/\beta_1$
3: $v_0 = 0$, $v_1 = b/\beta_1$
4: $\gamma_1 = \langle f(t), P_1(t)\rangle$
5: $z_1 = \gamma_1 v_1$
6: **for** $j = 1, \ldots, k$ **do**
7: $\quad \alpha_j = \langle tP_j(t), P_j(t)\rangle$
8: $\quad S_j(t) = tP_j(t) - \alpha_j P_j(t) - \beta_j P_{j-1}(t)$
9: $\quad \beta_{j+1} = \|S_j(t)\|$
10: $\quad P_{j+1}(t) = S_j(t)/\beta_{j+1}$
11: $\quad v_{j+1} = (Av_j - \alpha_j v_j - \beta_j v_{j-1})/\beta_{j+1}$
12: $\quad \gamma_{j+1} = \langle f(t), P_{j+1}(t)\rangle$
13: $\quad z_{j+1} = z_j + \gamma_{j+1} v_{j+1}$
14: **end for**
15: **return** $z_{k+1} \approx f(A)b$

3. Definition and computation of the inner products. Several points remain to be addressed to bring Algorithm 1 into a workable procedure. First, to compute the coefficients α_j, β_{j+1} and γ_{j+1}, we need to define an appropriate weight function w for the inner product (2.1). In addition, it is unlikely that numerical integration can be avoided if f is a truly arbitrary function. Therefore, the idea is to

replace f by a good approximation, preferably of spline type. We highlight below the strategy proposed in this paper for computing $f(A)b$:

> *First, approximate the function $f(t)$ by a spline $s(t)$. Then, use $s(t)$ in place of $f(t)$ in Algorithm 1 to compute the vector $z_{k+1} \approx s(A)b$, which in turn approximates $f(A)b$.*

Using splines in place of the original f yields many other benefits. Since a spline is nothing but a piecewise polynomial, inner products need to be computed on each subinterval only for polynomials. For this, a form of (exact) Gauss-Chebyshev quadrature will allow us to completely bypass numerical integration. In addition, splines can easily be adjusted to handle the problematic situation where the function f has "stiff" regions, by placing more knots in the places with high derivatives. This section provides the necessary implementation details of an algorithm based on this approach.

The cubic spline $s(t)$ is defined based on the knots $t_0 < t_1 < \cdots < t_{n-1} < t_n$:

$$s(t) := \sum_{i=0}^{n-1} s_i(t), \qquad t \in [l, u],$$

with $l = t_0$ and $t_n = u$, where for each i, the polynomial piece is

$$s_i(t) = \begin{cases} a_i + e_i(t - t_i) + c_i(t - t_i)^2 + d_i(t - t_i)^3 & \text{if } t \in [t_i, t_{i+1}], \\ 0 & \text{otherwise.} \end{cases} \tag{3.1}$$

3.1. Inner product and orthogonal basis. Consider the Chebyshev polynomials of the first kind defined for $|x| \le 1$, by $T_p(x) = \cos(p \cos^{-1} x)$. As is well known, these polynomials satisfy the three-term recurrence $T_{p+1}(x) = 2xT_p(x) - T_{p-1}(x)$, starting with $T_0(x) = 1$ and $T_1(x) = x$. They are also known to constitute a sequence of orthogonal polynomials on the interval $[-1, 1]$ with respect to the weight function $1/\sqrt{1 - x^2}$. If we denote by δ_j the Dirac function $\delta_j = 1$ iff $j = 0$, then we can write

$$\int_{-1}^{1} \frac{T_p(x)T_q(x)}{\sqrt{1 - x^2}}\, dx = \frac{\pi}{2} \left[\delta_{p-q} + \delta_{p+q}\right] .$$

For an interval $[t_i, t_{i+1}]$, we perform a change of variable

$$x^{(i)}(t) = \frac{2}{t_{i+1} - t_i} t - \frac{t_{i+1} + t_i}{t_{i+1} - t_i},$$

and we define the polynomials

$$C_p^{(i)}(t) := T_p(x^{(i)}(t)), \qquad t \in [t_i, t_{i+1}], \tag{3.2}$$

and the inner product

$$\langle g(t), h(t) \rangle_{[t_i, t_{i+1}]} := \int_{t_i}^{t_{i+1}} \frac{g(t)h(t)}{\sqrt{(t - t_i)(t_{i+1} - t)}}\, dt. \tag{3.3}$$

This change of variable has a significant implication: The $C_p^{(i)}(t)$'s are orthogonal on the interval $[t_i, t_{i+1}]$ with respect to the inner product defined above, namely,

$$\left\langle C_p^{(i)}(t), C_q^{(i)}(t) \right\rangle_{[t_i, t_{i+1}]} = \frac{\pi}{2} \left[\delta_{p-q} + \delta_{p+q}\right] . \tag{3.4}$$

With (3.3), we define the inner product of g and h on the whole interval $[l, u]$ as follows

$$\langle g(t), h(t)\rangle_{[l,u]} := \sum_{i=0}^{n-1} \langle g(t), h(t)\rangle_{[t_i,t_{i+1}]}.$$

The subscript $[l, u]$ will be dropped in the rest of the paper in order to conform with the notation in (2.1); that is, when we use the notation $\langle\cdot,\cdot\rangle$, we always mean the inner product on the whole interval $[l, u]$. The corresponding norm of a function g on the interval $[t_i, t_{i+1}]$ is $\|g(t)\|_{[t_i,t_{i+1}]} := \langle g(t), g(t)\rangle^{1/2}_{[t_i,t_{i+1}]}$, and the overall norm $\|\cdot\|$ on the interval $[l, u]$ as defined in (2.2) satisfies

$$\|g(t)\|^2 = \sum_{i=0}^{n-1} \|g(t)\|^2_{[t_i,t_{i+1}]}.$$

3.2. Computing α_j, β_{j+1}, and γ_{j+1}. With the definition of an inner product on each interval, we can exploit the orthogonality of the basis (cf. Equation (3.4)) to efficiently compute the inner products in Algorithm 1 by expanding the involved functions using the basis *in each interval.* This redundancy allow to bypass numerical integration by using what amounts to a Gauss-Chebyshev quadrature on each interval. The three-term recurrence (2.3) along with the standard relations of Chebyshev polynomials allows us to update the required expansions. This approach was described in [27] for the case of two intervals. For completeness, we briefly discuss the derivation of the formulas to compute α_j, β_{j+1}, and γ_{j+1} for the general case.

First we consider the computation of α_j. Let $P_j(t)$ be expressed in $[t_i, t_{i+1}]$ as

$$P_j(t) = \sum_{p=0}^{j-1} \mu_{pj}^{(i)} C_p^{(i)}(t), \qquad j \geq 1.$$

For now we assume that the coefficients $\mu_{pj}^{(i)}$ are known; an update formula will be derived later. We need to compute $\langle tP_j, P_j\rangle$, and we start by noting that $tP_j(t) = \sum_{p=0}^{j-1} \mu_{pj}^{(i)} tC_p^{(i)}(t)$. The usual recurrence relation of the Chebyshev polynomials shows that, in the interval $[t_i, t_{i+1}]$,

$$\begin{aligned} tC_p^{(i)}(t) &= \frac{t_{i+1}-t_i}{4} C_{p+1}^{(i)}(t) + \frac{t_{i+1}+t_i}{2} C_p^{(i)}(t) + \frac{t_{i+1}-t_i}{4} C_{p-1}^{(i)}(t), \qquad p \geq 1, \\ tC_0^{(i)}(t) &= \frac{t_{i+1}-t_i}{2} C_1^{(i)}(t) + \frac{t_{i+1}+t_i}{2} C_0^{(i)}(t). \end{aligned} \tag{3.5}$$

With the conventions that $\mu_{-1,j}^{(i)} = 0$ and $\mu_{pj}^{(i)} = 0$ for all $p \geq j$, this leads to

$$tP_j(t) = \frac{t_{i+1}-t_i}{4} \mu_{0j}^{(i)} C_1^{(i)}(t) + \sum_{p=0}^{j} \left(\frac{t_{i+1}-t_i}{4} \left(\mu_{p-1,j}^{(i)} + \mu_{p+1,j}^{(i)} \right) + \frac{t_{i+1}+t_i}{2} \mu_{pj}^{(i)} \right) C_p^{(i)}(t).$$

We define

$$\sigma_{pj}^{(i)} := \frac{t_{i+1}-t_i}{4} \left(\mu_{p-1,j}^{(i)} + \mu_{p+1,j}^{(i)} \right) + \frac{t_{i+1}+t_i}{2} \mu_{pj}^{(i)}, \qquad p = 0, \ldots, j. \tag{3.6}$$

Then $\alpha_j = \langle tP_j(t), P_j(t)\rangle = \sum_{i=0}^{n-1} \langle tP_j(t), P_j(t)\rangle_{[t_i,t_{i+1}]}$ becomes

$$\begin{aligned}\alpha_j &= \sum_{i=0}^{n-1} \left\langle \frac{t_{i+1}-t_i}{4}\mu_{0j}^{(i)}C_1^{(i)}(t) + \sum_{p=0}^{j}\sigma_{pj}^{(i)}C_p^{(i)}(t), \sum_{p=0}^{j-1}\mu_{pj}^{(i)}C_p^{(i)}(t)\right\rangle_{[t_i,t_{i+1}]} \\ &= \pi\sum_{i=0}^{n-1}\left(\sigma_{0j}^{(i)}\mu_{0j}^{(i)} + \frac{t_{i+1}-t_i}{8}\mu_{0j}^{(i)}\mu_{1j}^{(i)} + \frac{1}{2}\sum_{p=1}^{j}\sigma_{pj}^{(i)}\mu_{pj}^{(i)}\right). \end{aligned} \tag{3.7}$$

We now consider the computation of β_{j+1} starting with the case $j = 0$. Recall that in Algorithm 1 we define $S_j(t) = tP_j(t) - \alpha_j P_j(t) - \beta_j P_{j-1}(t)$. It is easy to see from (2.3) that $\beta_1^2 = \|S_0(t)\|^2 = \sum_{i=0}^{n-1}\|C_0(t)\|_{[t_i,t_{i+1}]}^2 = n\pi$. For $j \geq 1$, we have

$$\begin{aligned}\beta_{j+1}^2 &= \|S_j(t)\|^2 = \|tP_j(t) - \alpha_j P_j(t) - \beta_j P_{j-1}(t)\|^2 \\ &= \sum_{i=0}^{n-1}\left\| \frac{t_{i+1}-t_i}{4}\mu_{0j}^{(i)}C_1^{(i)}(t) + \sum_{p=0}^{j}\sigma_{pj}^{(i)}C_p^{(i)}(t) - \right. \\ &\qquad\qquad \left. \alpha_j\sum_{p=0}^{j-1}\mu_{pj}^{(i)}C_p^{(i)}(t) - \beta_j\sum_{p=0}^{j-2}\mu_{p,j-1}^{(i)}C_p^{(i)}(t)\right\|_{[t_i,t_{i+1}]}^2 \\ &= \sum_{i=0}^{n-1}\left\| \frac{t_{i+1}-t_i}{4}\mu_{0j}^{(i)}C_1^{(i)}(t) + \sum_{p=0}^{j}\left(\sigma_{pj}^{(i)} - \alpha_j\mu_{pj}^{(i)} - \beta_j\mu_{p,j-1}^{(i)}\right)C_p^{(i)}(t)\right\|_{[t_i,t_{i+1}]}^2. \end{aligned}$$

We define

$$\eta_{pj}^{(i)} := \sigma_{pj}^{(i)} - \alpha_j\mu_{pj}^{(i)} - \beta_j\mu_{p,j-1}^{(i)}, \qquad p = 0,\ldots,j. \tag{3.8}$$

Then

$$\beta_{j+1} = \sqrt{\pi\sum_{i=0}^{n-1}\left[{\eta_{0j}^{(i)}}^2 + \frac{1}{2}\left(\eta_{1j}^{(i)} + \frac{t_{i+1}-t_i}{4}\mu_{0j}^{(i)}\right)^2 + \frac{1}{2}\sum_{p=2}^{j}{\eta_{pj}^{(i)}}^2\right]}. \tag{3.9}$$

Furthermore, since $P_{j+1}(t) = S_j(t)/\beta_{j+1}$, we have the following update formula for $\mu_{p,j+1}^{(i)}$:

$$\mu_{p,j+1}^{(i)} = \begin{cases} \eta_{pj}^{(i)}/\beta_{j+1} & \text{if } p = 0,2,3,\ldots,j, \\ \left[\eta_{1j}^{(i)} + \frac{t_{i+1}-t_i}{4}\mu_{0j}^{(i)}\right]/\beta_{j+1} & \text{if } p = 1. \end{cases} \tag{3.10}$$

The initial condition is $\mu_{01}^{(i)} = 1/\beta_1$ for all i, since $P_1(t) = C_0(t)/\beta_1$.

Now consider γ_{j+1}. Since we use $s(t)$ in place of $f(t)$ in Algorithm 1, we have

$$\gamma_{j+1} = \langle s(t), P_{j+1}(t)\rangle = \sum_{i=0}^{n-1}\left\langle s_i(t), \sum_{p=0}^{j}\mu_{p,j+1}^{(i)}C_p^{(i)}(t)\right\rangle_{[t_i,t_{i+1}]}.$$

Note that $s_i(t)$ is a cubic polynomial; therefore, we have the expansion

$$s_i(t) = \xi_0^{(i)}C_0^{(i)}(t) + \xi_1^{(i)}C_1^{(i)}(t) + \xi_2^{(i)}C_2^{(i)}(t) + \xi_3^{(i)}C_3^{(i)}(t),$$

where $h_i = (t_{i+1} - t_i)/2$, and

$$\xi_0^{(i)} = \frac{5}{2}d_i h_i^3 + \frac{3}{2}c_i h_i^2 + e_i h_i + a_i, \quad \xi_2^{(i)} = \frac{3}{2}d_i h_i^3 + \frac{1}{2}c_i h_i^2,$$
$$\xi_1^{(i)} = \frac{15}{4}d_i h_i^3 + 2c_i h_i^2 + e_i h_i, \qquad \xi_3^{(i)} = \frac{1}{4}d_i h_i^3. \tag{3.11}$$

Thus,

$$\gamma_{j+1} = \pi \sum_{i=0}^{n-1} \left(\xi_0^{(i)} \mu_{0,j+1}^{(i)} + \frac{1}{2} \sum_{p=1}^{\min\{j,3\}} \xi_p^{(i)} \mu_{p,j+1}^{(i)} \right). \tag{3.12}$$

3.3. The final algorithm. Algorithm 2 is the final algorithm that incorporates the details just discussed. The orthogonal polynomials $P_j(t)$ do not appear explicitly. They are represented by their expansion coefficients in each interval. The scalars α_j, β_{j+1} and γ_{j+1} are now computed via the expansion coefficients $\sigma_{pj}^{(i)}$, $\eta_{pj}^{(i)}$, $\xi_p^{(i)}$, and $\mu_{pj}^{(i)}$. This approach avoids numerical integration, and the updates of the coefficients are simple. The only matrix-vector multiplication occurs in line 14, which involves the matrix A with a right-hand vector. Also, the function f is used only at the beginning of the algorithm, when an interpolating spline $s(t)$ is computed.

Algorithm 2 Approximating $f(A)b$, final version

Input: $t_0, t_1, \ldots, t_n$, where $t_0 = l$, $t_n = u$ and $t_i < t_{i+1}$ for all i
Input: number of steps k
1: Compute a cubic spline $s(t)$ which interpolates points $(t_i, f(t_i))$ for $i = 0, \ldots, n$, i.e., compute the coefficients a_i, e_i, c_i, d_i in (3.1).
2: $\beta_1 = \sqrt{n\pi}$
3: $v_1 = b/\beta_1$
4: Compute $\xi_p^{(i)}$ for $i = 0, \ldots, n-1$ and $p = 0, \ldots, 3$ using (3.11)
5: $\mu_{01}^{(i)} = 1/\beta_1$ for $i = 0, \ldots, n-1$
6: $\gamma_1 = \pi \sum_{i=0}^{n-1} \xi_0^{(i)} \mu_{01}^{(i)}$
7: $z_1 = \gamma_1 v_1$
8: **for** $j = 1, \ldots, k$ **do**
9: Compute $\sigma_{pj}^{(i)}$ for $i = 0, \ldots, n-1$ and $p = 0, \ldots, j$ using (3.6)
10: Compute α_j using (3.7)
11: Compute $\eta_{pj}^{(i)}$ for $i = 0, \ldots, n-1$ and $p = 0, \ldots, j$ using (3.8)
12: Compute β_{j+1} using (3.9)
13: Compute $\mu_{p,j+1}^{(i)}$ for $i = 0, \ldots, n-1$ and $p = 0, \ldots, j$ using (3.10)
14: $v_{j+1} = (Av_j - \alpha_j v_j - \beta_j v_{j-1})/\beta_{j+1}$
15: Compute γ_{j+1} using (3.12)
16: $z_{j+1} = z_j + \gamma_{j+1} v_{j+1}$
17: **end for**
18: **return** $z_{k+1} \approx f(A)b$

Let us analyze the computational costs of Algorithm 2, assuming that A is a sparse matrix of size $m \times m$. The time cost includes the time to perform a spline interpolation, which is linear to the number of knots n. The main body of the algorithm starting from line 2 has a cost of $O(k(kn + m + T_A))$, where T_A is the time for computing

a matrix-vector product between A and any right-hand vector. For each iteration, the portion kn comes from computing α_j, β_{j+1}, γ_{j+1}, and other coefficients, and the portion m comes from the length-m vector operations in lines 14 and 16.

In terms of storage costs, the dominant one is likely that of the matrix A, although there are applications where the matrix is used only in operator form. For the storage of other variables in the algorithm, note that only three m-dimensional vectors are needed for the v_j's and one vector for the latest z_j, leading to a total of $4m$ storage locations. In addition, we need to use $3kn$ locations to store $\mu_{p,j+1}^{(i)}$, $\mu_{pj}^{(i)}$, and $\mu_{p,j-1}^{(i)}$; kn locations to store $\sigma_{pj}^{(i)}$; and kn locations to store $\eta_{pj}^{(i)}$. We also need $4n$ locations to store $\xi_p^{(i)}$ and n locations to store h_i. These costs are summarized as $5kn + 5n + 4m$ locations.

So far, we have not discussed how to set t_i (which also determines the size of n). The choice of the knots is experimental and dependent on the function. A general guideline is that when the function derivative is large, we use short subintervals. This is important in order to obtain an accurate spline and the least squares polynomial. In Section 5, we propose a scheme that empirically works well for functions such as square root and logarithm. Also in Section 6.5 we briefly mention a scheme for the exponential function.

4. Convergence analysis. In Algorithm 2, we approximate $f(t)$ on the interval $[l, u]$ by a cubic spline $s(t)$, and we project $s(t)$ onto the polynomial space $\mathbb{P}_{k+1}$, which consists of polynomials of degree not exceeding k:

$$s(t) \approx \sum_{j=1}^{k+1} \gamma_j P_j(t) := \phi_{k+1}(t), \tag{4.1}$$

where $\{P_j(t)\}$ is an orthonormal basis of $\mathbb{P}_{k+1}$, with

$$\gamma_j = \langle s(t), P_j(t) \rangle .$$

The approximant is

$$z_{k+1} := \phi_{k+1}(A)b.$$

By way of introduction we present the following easy-to-prove or well-known results.

PROPOSITION 4.1. *For the norm $\|\cdot\|$ defined earlier (cf. Equation (2.2) and Section 3.1),*

$$\phi_{k+1}(t) = \arg \min_{\phi \in \mathbb{P}_{k+1}} \|\phi(t) - s(t)\| . \tag{4.2}$$

In addition, if A is symmetric and its spectrum is included in $[l, u]$, then

$$\|z_{k+1} - f(A)b\|_2 \leq \max_{t \in [l,u]} |\phi_{k+1}(t) - f(t)| \, \|b\|_2 . \tag{4.3}$$

Proof. The first result is well known for least squares approximations. The second comes from the fact that A can be written as $A = VDV^T$, where V is unitary, and follows trivially by expanding $z_{k+1} - f(A)b = (\phi_{k+1}(A) - f(A))b$ in the eigenbasis. ∎

To bound the difference between $\phi_{k+1}(t)$ and $f(t)$ on the interval $[l, u]$, note that

$$|\phi_{k+1}(t) - f(t)| \leq |\phi_{k+1}(t) - s(t)| + |s(t) - f(t)| .$$

Hence, we need to estimate the two terms on the right-hand side of the above inequality separately. For the second term, many known error bounds for splines can be exploited. The following presents a standard result for clamped cubic splines, which indicates a fourth-order accuracy.

THEOREM 4.2 ([31, pp. 57–58]). *If $f(t)$ is fourth-order differentiable on the interval $[l, u]$ and if $s(t)$ is the unique cubic spline that interpolates $f(t)$ on the knots $l = t_0 < t_1 < \cdots < t_n = u$ with the boundary condition*

$$s'(t_0) = f'(t_0) \qquad \text{and} \qquad s'(t_n) = f'(t_n),$$

then

$$\max_{t\in[l,u]} |s(t) - f(t)| \leq \frac{5M}{384} \max_{0\leq i\leq n-1} (t_{i+1} - t_i)^4,$$

where $M = \max_{t\in[l,u]} \left|f^{(4)}(t)\right|$.

To bound the difference $|\phi_{k+1}(t) - s(t)|$, we need the following two lemmas. They are extensions of similar results given in [27], and hence the proofs are omitted.

LEMMA 4.3. *Using the notation of a function norm $\|\cdot\|$ in this paper, we have*

$$\|g(t)\| \leq \sqrt{n\pi} \cdot \max_{t\in[l,u]} |g(t)| .$$

LEMMA 4.4. *Let $g_{k+1}(t) \in \mathbb{P}_{k+1}$ be any polynomial of degree not exceeding k. Then, using the notation of a function norm $\|\cdot\|$ in this paper, we have*

$$\max_{t\in[l,u]} |g_{k+1}(t)| \leq \sqrt{\frac{2(k+1)}{\pi}} \|g_{k+1}(t)\| .$$

By a property of the uniform norm, for any continuous function $g(t)$, there exists a degree-k polynomial $g^*_{k+1}(t)$ such that

$$\max_{t\in[l,u]} \left|g^*_{k+1}(t) - g(t)\right| \leq \max_{t\in[l,u]} |\phi(t) - g(t)| , \qquad \forall \phi \in \mathbb{P}_{k+1}.$$

The *modulus of continuity* of a function $g(t)$ on the interval $[l, u]$ is defined for all $\delta > 0$,

$$\omega(g; [l, u]; \delta) := \sup_{\substack{t_1,t_2\in[l,u] \\ |t_1-t_2|\leq\delta}} |g(t_1) - g(t_2)| .$$

We use the shorthand notation $\omega(\delta)$ when the context is clear. The following is a corollary of the Jackson's theorem for bounding the uniform approximation of a function g.

LEMMA 4.5 ([26, Corollary 1.4.1, p. 22]). *If $g \in C[l, u]$, then*

$$\max_{t\in[l,u]} \left|g^*_{k+1}(t) - g(t)\right| \leq 6\omega\left(\frac{u-l}{2k}\right).$$

The above lemmas lead to the following theorem, which gives an upper bound for the convergence rate of $\phi_{k+1}(t)$ to $s(t)$.

THEOREM 4.6. *The uniform norm of the residual polynomial admits the following bound:*

$$\max_{t\in[l,u]} |\phi_{k+1}(t) - s(t)| \leq 6(2\sqrt{2n(k+1)}+1)\omega\left(\frac{u-l}{2k}\right). \tag{4.4}$$

Proof. We have

$$\max_{t\in[l,u]} |\phi_{k+1}(t) - s(t)| \leq \max_{t\in[l,u]} \left|\phi_{k+1}(t) - s^*_{k+1}(t)\right| + \max_{t\in[l,u]} \left|s^*_{k+1}(t) - s(t)\right|. \tag{4.5}$$

From Lemma 4.4,

$$\max_{t\in[l,u]} \left|\phi_{k+1}(t) - s^*_{k+1}(t)\right| \leq \sqrt{\frac{2(k+1)}{\pi}} \left\|\phi_{k+1}(t) - s^*_{k+1}(t)\right\|. \tag{4.6}$$

Since

$$\begin{aligned}\left\|\phi_{k+1}(t) - s^*_{k+1}(t)\right\| &\leq \|\phi_{k+1}(t) - s(t)\| + \left\|s(t) - s^*_{k+1}(t)\right\| \\ &\leq \left\|s^*_{k+1}(t) - s(t)\right\| + \left\|s(t) - s^*_{k+1}(t)\right\| \qquad \text{(by Eqn. (4.2))} \\ &= 2\left\|s^*_{k+1}(t) - s(t)\right\|, \end{aligned} \tag{4.7}$$

the inequality (4.6) becomes

$$\max_{t\in[l,u]} \left|\phi_{k+1}(t) - s^*_{k+1}(t)\right| \leq 2\sqrt{\frac{2(k+1)}{\pi}} \left\|s^*_{k+1}(t) - s(t)\right\|.$$

Recall from Lemma 4.3 that $\left\|s^*_{k+1}(t) - s(t)\right\| \leq \sqrt{n\pi}\max_{t\in[l,u]} \left|s^*_{k+1}(t) - s(t)\right|$. Therefore,

$$\max_{t\in[l,u]} \left|\phi_{k+1}(t) - s^*_{k+1}(t)\right| \leq 2\sqrt{2n(k+1)} \max_{t\in[l,u]} \left|s^*_{k+1}(t) - s(t)\right|.$$

Thus, (4.5) becomes

$$\max_{t\in[l,u]} |\phi_{k+1}(t) - s(t)| \leq (2\sqrt{2n(k+1)}+1) \max_{t\in[l,u]} \left|s^*_{k+1}(t) - s(t)\right|.$$

The theorem is established by applying Lemma 4.5. ∎

A function $g(t)$ defined on $[l,u]$ is ν-Lipschitz with constant K if

$$|g(t_1) - g(t_2)| \leq K\,|t_1 - t_2|^{\nu}, \qquad \forall t_1, t_2 \in [l,u].$$

We have the following corollary for Theorem 4.6.

COROLLARY 4.7. *Let $s(t)$ be ν-Lipschitz with constant K. Then,*

$$\max_{t\in[l,u]} |\phi_{k+1}(t) - s(t)| \leq 6K\left(\frac{u-l}{2}\right)^{\nu} \frac{2\sqrt{2n(k+1)}+1}{k^{\nu}} = O\left(\frac{1}{k^{\nu-1/2}}\right). \tag{4.8}$$

We remark that the bound (4.8) may sometimes be too pessimistic. However, it does suggest two facts for understanding the convergence of $\phi_{k+1}(t)$. First, the asymptotic rate $O(1/k^{\nu-1/2})$ fits the observed practical behavior. Numerical results will later show that in the log-log scale, the uniform norm decays like a straight line.

In other words, empirically, we can fit some constants $c_1 > 0$ and c_2 such that (see Section 6.2)

$$\log\left(\max|\phi_{k+1}(t) - s(t)|\right) \approx -c_1 \log k + c_2.$$

The second useful fact is that when $s(t)$ has a large derivative (i.e., K is large) and/or is defined on a long interval (i.e., $u - l$ is large), then the observed error will also be large. This makes approximating some functions such as the square root challenging. On the one hand, if the largest eigenvalue of A is moderate whereas the smallest eigenvalue is close to zero, then K will be very large. On the other hand, if we scale the matrix such that the smallest eigenvalue is away from zero, then the spectrum will span a very long interval.

Apart from the above result for the uniform norm of $\phi_{k+1}(t) - s(t)$, we can also give a bound for its norm.

THEOREM 4.8. *The norm of the residual polynomial admits the following bound:*

$$\|\phi_{k+1}(t) - s(t)\| \leq 18\sqrt{n\pi}\omega\left(\frac{u-l}{2k}\right).$$

Proof. This follows from

$$\begin{aligned}
\|\phi_{k+1}(t) - s(t)\| &\leq \left\|\phi_{k+1}(t) - s^*_{k+1}(t)\right\| + \left\|s^*_{k+1}(t) - s(t)\right\| \\
&\leq 3\left\|s^*_{k+1}(t) - s(t)\right\| && \text{(by (4.7))} \\
&\leq 3\sqrt{n\pi}\max_{t\in[l,u]}\left|s^*_{k+1}(t) - s(t)\right| && \text{(by Lemma 4.3)} \\
&\leq 18\sqrt{n\pi}\omega\left(\frac{u-l}{2k}\right). && \text{(by Lemma 4.5)}
\end{aligned}$$

□

From the above result one can trivially obtain a bound analogous to that of Corollary 4.7 for the case when $s(t)$ is ν-Lipschitz with constant K:

$$\|\phi_{k+1}(t) - s(t)\| \leq 18K\left(\frac{u-l}{2}\right)^{\nu}\frac{\sqrt{n\pi}}{k^{\nu}} = O\left(\frac{1}{k^{\nu}}\right). \tag{4.9}$$

5. Application: computing $A^{1/2}b$. We consider a case where $f(t)$ is the square root function and A is symmetric positive definite. We note that the symmetry requirement of A is not necessary; A only needs to be diagonalizable with all its eigenvalues positive. Further, the positive definiteness requirement of A can be relaxed to positive semi-definiteness. This will affect only the choice of the interval $[l, u]$ (cf. Section 5.2), which needs to contain only the nonzero eigenvalues of A.

5.1. Background and challenge. Sampling from a multivariate Gaussian distribution with a positive definite covariance matrix $K \in \mathbb{R}^{m\times m}$ is one of the most common endeavors in statistics. The most common approach is to compute the Cholesky factorization $K = LL^T$, where L is a lower triangular matrix. If x is a vector whose entries are independent and are normally distributed with mean 0 and variance 1, that is, $x \sim \mathcal{N}(\mathbf{0}_m, \mathbb{I}_m)$, then $\zeta = \mathbf{m} + Lx$ is a random variable whose distribution is $\mathcal{N}(\mathbf{m}, K)$. Many modern applications often require high-fidelity spatio temporal sampling, which puts m in the range of 10^{12}–10^{15}. This results in the need to identify sampling approaches that have both $O(m)$ complexity and high potential for parallelism.

If the sample sites are on a regular grid and the covariance function is stationary, then several techniques can be used to sample efficiently from the Gaussian distribution. One can use specialized linear algebra to carry out the Cholesky factorization, at least for some one-dimensional problems for a number of sampling sites up to 10^6 [12]. Other possibilities are to use a multigrid-type sampling scheme, Galerkin multigrid Monte Carlo (MGMC) [15], or to embed the covariance matrix in a stationary periodic process [8], followed by a fast Fourier transformation (FFT) technique.

Nevertheless, none of these approaches was demonstrated to work for the case where the data points are not on a regular grid, or for nonstationary covariance functions, or on the scale of problems that we aim to solve. In the case of the structured Cholesky approach of [12], it is unclear whether an indexing can be found that will result in sufficient sparsity of the factors for the non regular grid, nonstationary covariance function, or multiple dimensions. In addition, at extremely large numbers of sites, Cholesky factorization cannot be expected to be as efficient to parallelize as a matrix-free approach. The FFT approach may be difficult to parallelize beyond a thousand processors [4]. More important perhaps, even for small processor counts, FFT cannot be applied when the sampling sites are not on a regular grid or the Gaussian process is not stationary. For MGMC, the compact kernel has much larger bandwidth than do the covariance matrices for which they are traditionally applied, which are of the Laplace-matrix type [15]. This situation may result in rapid densification and increase in storage requirements [11] [33, §7.7.5].

Many examples of interest need to sample the Gaussian process at points that cannot be easily embedded in a regular grid. For example, the positions of windfarms or their wind turbines cannot be easily approximated with a grid, unless the grid cell is exceedingly small [5]. In geostationary applications, the spherical shape of the Earth prevents most spatial grids of interest from being regular when projected on a plane. Moreover, there are countless examples of nonstationary Gaussian processes of interest [32, 25] for which FFT cannot work, and neither Cholesky nor MGMC approaches were demonstrated.

We therefore turn to an entirely matrix-free approach for computing $K^{1/2}x$. If $x \sim \mathcal{N}(\mathbf{0}_m, \mathbb{I}_m)$ then $\eta = \mathbf{m} + K^{1/2}x$ is a random variable whose distribution is also $\mathcal{N}(\mathbf{m}, K)$. We thus achieve a matrix-free approach of sampling from an arbitrary normal distribution, irrespective of the positions of the sampling sites or the lack of stationarity in the covariance function that generates K.

Nevertheless, in order for the approach to have an $O(m)$ behavior, the matrix-vector multiplications must take $O(m)$ themselves. Therefore the covariance matrix K must be sparse. We will thus be interested primarily in covariance matrices originating in Gaussian processes with compact kernels. Such processes are widely used in applications and result in sparse covariance matrices [25]. In addition, it is sometimes possible to replace K by the covariance matrix obtained from a compact kernel with little bias or loss of statistical efficiency compared to the original covariance function [19, 12].

5.2. The interval $[l, u]$. We now consider further details to carry out Algorithm 2 specifically for the square root function. One issue is the interval $[l, u]$, which needs to contain the spectrum of A. By Theorem 4.2, the subintervals $[t_i, t_{i+1}]$ should be small enough to yield an accurate spline $s(t)$. However, too many intervals will impose a heavy computational burden, for both the spline approximation and the computation of the coefficients α_j, β_{j+1} and γ_{j+1}. On the other hand, the closer zero is to the interval, the harder it is to interpolate $\sqrt{t}$, since the tangent tends to infinity.

A geometric progression of the spacing between the knots works well in practice, so we opt to let

$$t_0 = \lambda_{\min}/(1+a), \qquad t_i = (1+a)^i t_0, \qquad i = 1, 2, \ldots, n,$$

and to let t_n be some value such that $t_n \geq \lambda_{\max}$, where $\lambda_{\min}$ and $\lambda_{\max}$ are the smallest and the largest eigenvalue of A, respectively. From this we have

$$n = \left\lceil \log_{1+a} \frac{\lambda_{\max}}{\lambda_{\min}} \right\rceil + 1 = \left\lceil \log_{1+a} \kappa \right\rceil + 1,$$

where κ is the 2-norm condition number of A. We choose $a = 0.01$. Note that this interval scheme requires an estimate of the two extreme eigenvalues of A. We avoid using $t_0 = \lambda_{\min}$ when the estimate is not accurate enough.

5.3. Convergence test. As shown in the analysis in Section 4, the convergence of z_{k+1} to $f(A)b$ can be split in two parts: the convergence of the spline $s(t)$ to $f(t)$ and the convergence of the least squares approximation $\phi_{k+1}(t)$ to $s(t)$. The spline is usually a sufficiently good approximation to $f(t)$ if one uses the intervals designed in Section 5.2. Therefore, we consider mainly the approximation quality of $\phi_{k+1}(t)$.

As discussed after Corollary 4.7, the bound (4.8) is not useful for determining an appropriate k. Instead, a natural heuristic is to consider the difference of consecutive iterates

$$\frac{\|z_{k+1} - z_k\|_2}{\|z_{k+1}\|_2} \tag{5.1}$$

and ensure that it falls below a certain tolerance ϵ.

Another possible criterion is to check the norm of the residual polynomial:

$$\frac{\|s(t) - \phi_{k+1}(t)\|}{\|s(t)\|}. \tag{5.2}$$

Lemmas 4.3 and 4.5 suggest that the norm of $s(t) - \phi_{k+1}(t)$ should decay similarly to that of the uniform norm. Since $\phi_{k+1}(t)$ is a least squares approximation, we have

$$\|s(t) - \phi_{k+1}(t)\|^2 = \|s(t)\|^2 - \|\phi_{k+1}(t)\|^2.$$

Therefore, the relative difference (5.2) can be easily computed by noting that

$$\|s(t)\|^2 = \sum_{i=0}^{n} \left[\left(\xi_0^{(i)}\right)^2 \pi + \left(\xi_1^{(i)}\right)^2 \frac{\pi}{2} + \left(\xi_2^{(i)}\right)^2 \frac{\pi}{2} + \left(\xi_3^{(i)}\right)^2 \frac{\pi}{2} \right] \quad \text{and} \quad \|\phi_{k+1}(t)\|^2 = \sum_{j=1}^{k+1} \gamma_j^2.$$

However, numerical experiments indicate that (5.1) is more appropriate than (5.2) as a criterion for the convergence test; see Section 6.1.

We point out that for the problem of sampling from a Gaussian distribution as discussed in Section 5.1, another possibility emerges for estimating the error. Since $\eta = \mathbf{m} + K^{1/2}x$ and the approximant $\hat{\eta} = \mathbf{m} + \phi_{k+1}(K)x$, we have

$$\eta^\epsilon = \eta - \hat{\eta} = (K^{1/2} - \phi_{k+1}(K))x.$$

If $x \sim \mathcal{N}(\mathbf{0}_m, \mathbb{I}_m)$, then it is easy to see that η^ϵ is normally distributed with mean 0 and variance $\mathbf{Var}(\eta^\epsilon) = K - 2K^{1/2}\phi_{k+1}(K) + \phi_{k+1}^2(K)$. From inequality (4.3) it follows that

$$\sqrt{\|\mathbf{Var}(\eta^\epsilon)\|_2} \leq \max_{t \in [l,u]} |\phi_{k+1}(t) - f(t)|. \tag{5.3}$$

The right-hand side of the above bound can then be used for statistical tests characterizing the discrepancy between the approximant $\hat{\eta}$ and the variable η that has the exact sought-after distribution. This uniform norm can be empirically estimated by a large enough sampling $\{\hat{t}_i\}$ of the interval $[l, u]$. (Note the $\hat{t}_i$'s are different from the knots t_i's.) To compute $\phi_{k+1}(t)$, note that the vector $[\phi_{k+1}(\hat{t}_1), \ldots, \phi_{k+1}(\hat{t}_r)]^T$ is indeed the output $\hat{z}_{k+1}$ of Algorithm 2 from a diagonal matrix $\hat{A} = \mathrm{diag}(\hat{t}_1, \ldots, \hat{t}_r)$ with the right-hand vector $\hat{b}$, which is the vector of all 1's. In other words, one needs to replicate lines 14 and 16 with a second set of matrix $\hat{A}$ and vectors $\hat{v}_j$ and $\hat{z}_j$. When $\hat{A}$ is large, this additional computation might be expensive, although its cost is independent of the size of the original matrix A and thus, on the number of sampling sites, which tends to dominate all other sizes involved.

6. Numerical results. In this section, we show several numerical experiments to demonstrate the effectiveness and scalability of Algorithm 2. Note an important relation for a symmetric matrix A:

$$\|\phi_{k+1}(A)b - f(A)b\|_2 = \left\|V\phi_{k+1}(D)V^Tb - Vf(D)V^Tb\right\|_2 = \left\|\phi_{k+1}(D)\tilde{b} - f(D)\tilde{b}\right\|_2,$$

where $V^TAV = D$ is a diagonalization of A with a unitary V, and $\tilde{b} = V^Tb$. This means that if the right-hand vector b is drawn from some distribution (such as uniform or $\mathcal{N}(\mathbf{0}_m, \mathbb{I}_m)$), then the approximation error for computing $f(A)b$ is equal to that for computing $f(D)\tilde{b}$, where $\tilde{b}$ can be considered a sample from the same distribution. In other words, in a statistical sense, testing a matrix A is equivalent to testing the diagonal matrix D, which has the same spectrum as A. An advantage of this replacement is that the ground truth $f(D)b$ is much easier to compute than $f(A)b$. Therefore, all the experiments here were performed on the diagonal matrix D which is unitarily similar to the original A unless otherwise noted. Also, except for the last subsection, all the experiments were performed for the square root function $f(t) = t^{1/2}$.

6.1. Tests on matrices from the UF collection. We first tested the proposed algorithm on a set of symmetric positive definite matrices from the UF sparse matrix collection [7]. We chose these matrices with a moderate size m and from ten different application domains, including statistics, materials, power networks, and structural problems. Table 6.1 lists the matrices and the numerical results. For convenience, we list the matrices in the increasing order of their condition numbers κ. The middle column shows the spline-fitting error, $\max_{t\in\Lambda(A)} |s(t) - f(t)|$, which indicates that the spline is in general a sufficiently good approximation to the original function. In the experiment, we set the maximum number of iterations k to be 200 and the tolerance (cf. Equation (5.1)) to be 10^{-6}. The final residual

$$\frac{\left\|z_{k+1} - A^{1/2}b\right\|}{\left\|A^{1/2}b\right\|}$$

is listed in the last column. We can see that as the condition number of the matrix increases, the approximation in general becomes less accurate. In other words, the polynomial approximation is affected by the conditioning of the matrix. We can also see that the tolerance is only a few times away from the residual, which implies that it can serve as a suitable criterion of the convergence and a good estimate of the actual residual.

TABLE 6.1
Numerical results on the matrices from the UF collection.

Group/Name	κ	Spline Err.	k	Tolerance	Residual
`Boeing/crystm01`	2.28×10^{2}	5.20×10^{-16}	52	9.60×10^{-7}	1.28×10^{-6}
`Bates/Chem97ZtZ`	2.47×10^{2}	8.35×10^{-9}	57	9.37×10^{-7}	4.07×10^{-6}
`JGD/Trefethen_2000`	1.55×10^{4}	3.43×10^{-8}	200	5.80×10^{-6}	4.41×10^{-6}
`TKK/plbuckle`	1.28×10^{6}	3.53×10^{-7}	200	1.08×10^{-4}	2.87×10^{-4}
`Nasa/nasa1824`	1.89×10^{6}	1.12×10^{-6}	200	1.37×10^{-4}	1.26×10^{-3}
`HB/1138_bus`	8.57×10^{6}	3.31×10^{-8}	200	1.94×10^{-4}	1.51×10^{-3}
`Oberwolfach/t2dal_e`	3.76×10^{7}	2.70×10^{-13}	200	1.59×10^{-4}	6.55×10^{-4}
`HB/bcsstk12`	2.21×10^{8}	1.93×10^{-6}	200	2.18×10^{-4}	1.24×10^{-3}
`FIDAP/ex3`	1.68×10^{10}	1.04×10^{-6}	200	1.88×10^{-4}	1.06×10^{-3}
`Bai/mhd3200b`	1.60×10^{13}	3.54×10^{-10}	200	4.73×10^{-4}	4.61×10^{-3}

We performed a further investigation on the matrices of the best (`crystm01`) and the worst (`mhd3200b`) performance (see Figure 6.1). Plot (a) shows three curves as k increases: the residual, the tolerance (Equation (5.1)), and the norm of the residual polynomial (Equation (5.2)). This plot shows an advantage of using (5.1) rather than (5.2) as the convergence criterion. It suggests that numerically the norm will stop decreasing far before the uniform norm does. Of course, this may affect well-conditioned matrices only, since for ill-conditioned matrices (cf. Plot (b)), within a reasonable number of iterations, say 200, neither norm appears to stop decreasing. To further expose the distribution of the errors, plots (b) and (d) show the value of the residual polynomial $|\phi_{k+1}(t) - s(t)|$ for t equal to the eigenvalues. As expected, the smallest eigenvectors do not seem to contribute in a major way to the residual.

6.2. Scalability. We tested the scalability performance of the algorithm on two types of matrices: "uniform" and "lap2D" . A "uniform" matrix of size $m \times m$ is a diagonal matrix with diagonal entries i/m, $i = 1, 2, \ldots, m$. The condition number is $\kappa = m$. A "lap2D" matrix is the standard Laplacian on a uniform $m_1 \times m_2$ grid. It is of size $m = m_1.m_2$ and is given by

$$\begin{bmatrix} A & -I & & & \\ -I & A & -I & & \\ & \ddots & \ddots & \ddots & \\ & & -I & A & -I \\ & & & -I & A \end{bmatrix}_{m\times m} \quad \text{with} \quad A = \begin{bmatrix} 4 & -1 & & & \\ -1 & 4 & -1 & & \\ & \ddots & \ddots & \ddots & \\ & & -1 & 4 & -1 \\ & & & -1 & 4 \end{bmatrix}_{m_1\times m_1}.$$

The eigenvalues of lap2D are known:

$$4\left[\sin^2\left(\frac{i\pi}{2(m_1+1)}\right) + \sin^2\left(\frac{j\pi}{2(m_2+1)}\right)\right], \quad i = 1, \ldots, m_1, \;\; j = 1, \ldots, m_2.$$

Therefore, its condition number is

$$\kappa = \frac{\sin^2\left(\frac{m_1\pi}{2(m_1+1)}\right) + \sin^2\left(\frac{m_2\pi}{2(m_2+1)}\right)}{\sin^2\left(\frac{\pi}{2(m_1+1)}\right) + \sin^2\left(\frac{\pi}{2(m_2+1)}\right)} \approx \frac{8/\pi^2}{1/m_1^2 + 1/m_2^2}.$$

When $m_1 = m_2 = \sqrt{m}$, it follows that $\kappa = O(m)$. Therefore, both types of matrices have a condition number on the order of their matrix sizes. Note also that in this

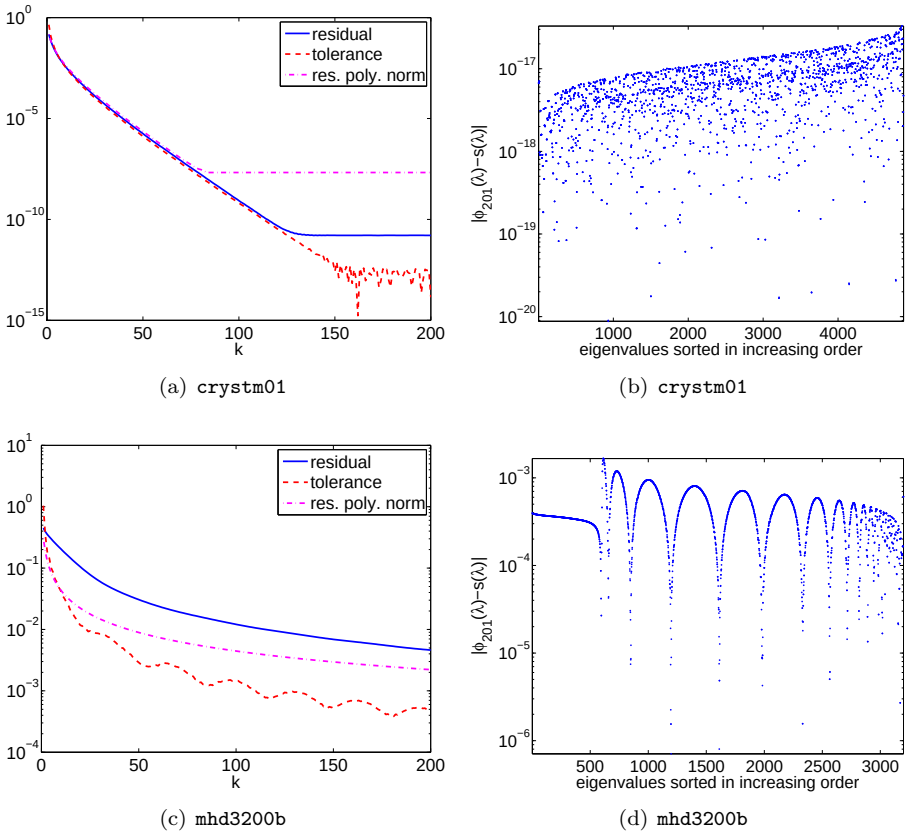

(a) `crystm01` (b) `crystm01`

(c) `mhd3200b` (d) `mhd3200b`

FIG. 6.1. *Residual plots for two matrices:* `crystm01` *and* `mhd3200b`.

case the number of knots n is

$$O(\log_{1+a} \kappa) = O(\log_{1+a} m).$$

Figure 6.2 shows a residual plot, a plot of the uniform norm of the residual polynomial as k increases, and a plot of the run time as m increases, for each type of matrix. The final residual with $k = 100$ iterations reached 10^{-5} to 10^{-4}. The uniform norm of the residual polynomial was empirically evaluated as

$$\max_{t \in \Lambda(A)} |\phi_{k+1}(t) - s(t)|,$$

for the largest matrix (i.e., $m = 10^8$). A log-log plot of this uniform norm versus the number of iterations shows a straight-line pattern. We fit a line to the plot, and the tangent was close to -1. This confirms the rate of convergence given in Corollary 4.7 for the uniform norm of $\phi_{k+1}(t) - s(t)$.

We also plotted the running time of the algorithm (see plots (e) and (f)), in log-log scale. The time included all the computations except the estimation of $\lambda_{\min}$ and $\lambda_{\max}$. Since the algorithm was implemented in Matlab as a serial program, we expect that a more careful implementation in C and/or in a parallel fashion will yield several folds or even magnitudes of time improvement. It can be seen from both plots that

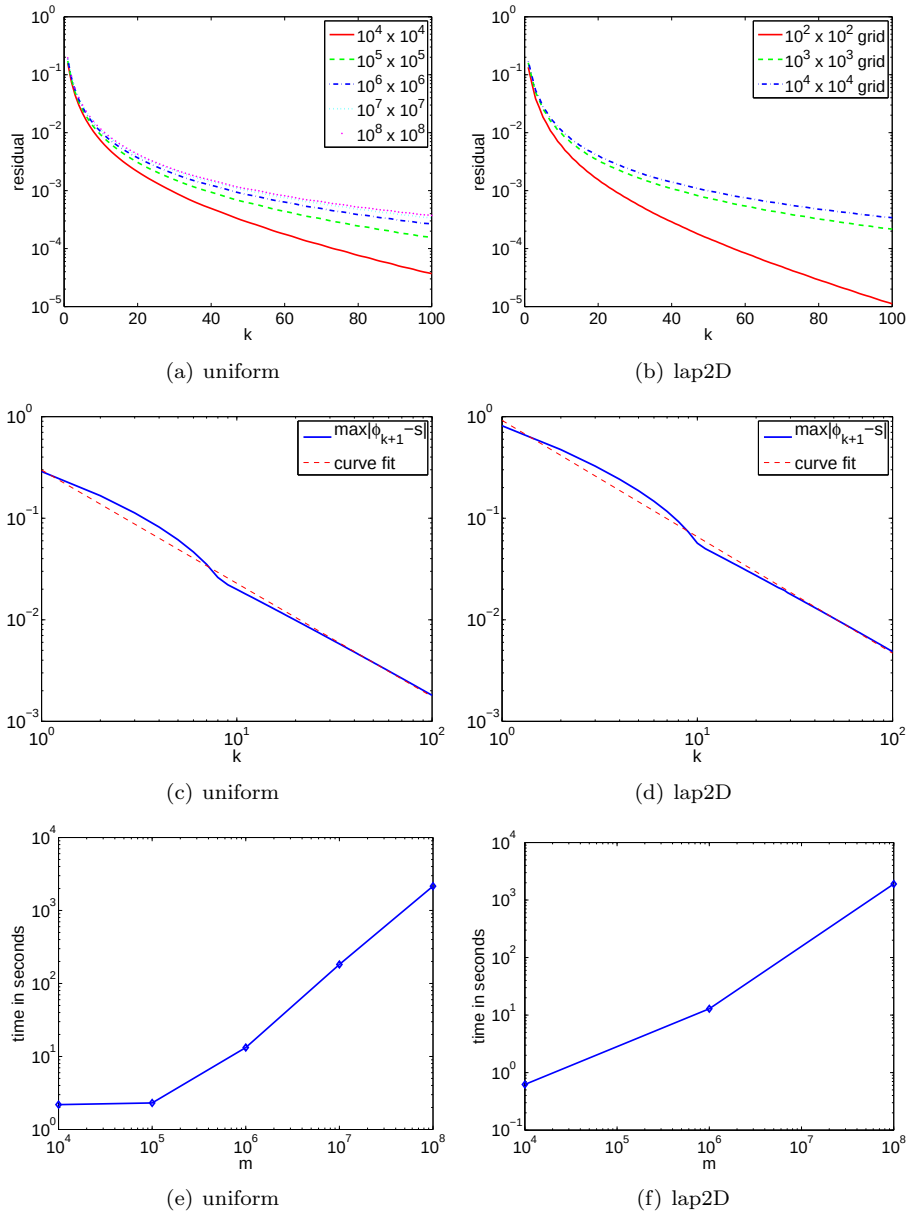

(a) uniform (b) lap2D

(c) uniform (d) lap2D

(e) uniform (f) lap2D

FIG. 6.2. *Numerical results on "uniform" matrices and "lap2D" matrices.*

the running time is linear as m increases, which is expected from the computational cost analysis.

6.3. Tests on a Gaussian process sampling problem. We consider the covariance matrix K mentioned in Section 5.1, originating in covariance functions with compact kernels described in [30, 25]. Such functions describe processes that can be used in the study of vehicles moving on terrains with random slip coefficients. The

covariance function has radial symmetry and rule

$$k(r) = \left(1 - \frac{r}{\alpha}\right)_+^{\beta}, \quad \text{where} \quad r = \sqrt{x^2 + y^2}.$$

The covariance matrix K therefore is defined on a 2D grid, with the (i, j) entry $K_{ij} = k(d_{ij})$, where d_{ij} is the Euclidean distance between two grid points.

To gauge the effects of the computations at sites that are not necessarily on a regular grid, we also consider the covariance matrix over a deformed space. In this case,

$$r = \sqrt{x^2 + w(x)y^2},$$

where $w(x)$ is a quadratic deforming function that is 2 in the middle of the range of x and 1 at its extremes. With this new definition, $k(r)$ can be looked at as either a nonstationary covariance function or a stationary covariance function on the grid shown in Figure 6.3. Neither case can be treated by the FFT approach [8].

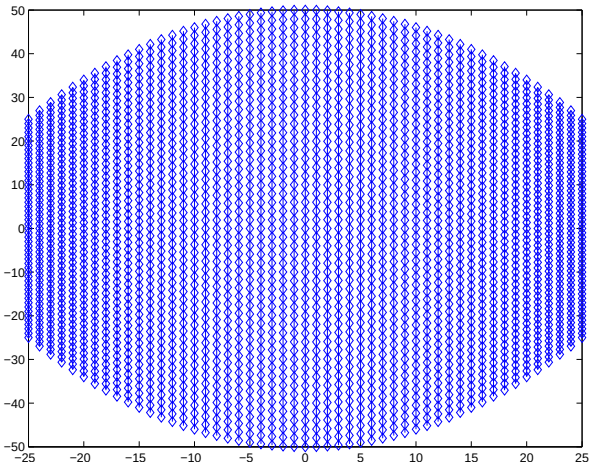

FIG. 6.3. *Position of sampling points in the non uniform grid case.*

We performed tests on the covariance matrices defined on both types of grids with different parameters, as listed in Table 6.2. "Regular" means the grid is uniform, with grid points separated with a spacing 1 unit; "deformed" means the grid is deformed as in Figure 6.3. The middle column shows the condition number κ, which suggests that a smaller α and a larger β will make the matrix better conditioned, and correspondingly the required vector $K^{1/2}b$ will be easier to compute. It also suggests that problems without a regular grid structure can be as easy to solve as the problems on a regular grid by our method. In general, within 100 iterations, the final residual has decreased to 10^{-10}–10^{-11}.

We performed further tests on larger grids, which imposed a difficulty for computing the ground truth $K^{1/2}b$ and the residual. We therefore presented only the tolerance and the empirical uniform norm of $\phi_{k+1}(t) - f(t)$. From Table 6.2 one sees that the tolerance is a good indication of the residual, and (5.3) implies that the uniform norm bounds the variance. To make the computation more feasible, we did not explicitly store the matrix; any matrix-vector multiplication was carried out by considering the special structure of K. Compared with Table 6.2, the results in Table 6.3

TABLE 6.2
Numerical results on the covariance matrices.

Grid	Grid Size	α	β	κ	k	Tolerance	Residual
Regular	100×100	6.5	3	35.10	49	8.0104×10^{-11}	1.2719×10^{-10}
Regular	100×100	12.5	3	243.59	120	9.5001×10^{-11}	4.2465×10^{-10}
Regular	100×100	6.5	5	13.13	31	6.6332×10^{-11}	5.6348×10^{-11}
Regular	100×100	12.5	5	88.01	75	8.8254×10^{-11}	2.3085×10^{-10}
Deformed	100×100	6.5	3	15.95	34	6.3934×10^{-11}	6.9053×10^{-11}
Deformed	100×100	12.5	3	107.10	82	9.0078×10^{-11}	2.6602×10^{-10}
Deformed	100×100	6.5	5	6.20	21	9.2292×10^{-11}	4.9578×10^{-11}
Deformed	100×100	12.5	5	38.65	51	9.2313×10^{-11}	1.5885×10^{-10}

suggest that the grid size has little impact on the conditioning of the matrices, and therefore the approximation quality was as good as for smaller grids.

TABLE 6.3
Numerical results on the covariance matrices.

Grid	Grid Size	α	β	κ	k	Tolerance	$\max\lvert\phi_{k+1}-f\rvert$
Regular	$10^3\times10^3$	6.5	3	35.14	48	9.5703×10^{-11}	1.2106×10^{-9}
Regular	$10^3\times10^3$	12.5	3	244.47	122	7.9481×10^{-11}	1.9733×10^{-9}
Regular	$10^3\times10^3$	6.5	5	13.14	32	5.6690×10^{-11}	4.2998×10^{-10}
Regular	$10^3\times10^3$	12.5	5	88.23	79	8.3043×10^{-11}	1.2952×10^{-9}
Deformed	$10^3\times10^3$	6.5	3	15.96	34	4.5546×10^{-11}	4.0252×10^{-10}
Deformed	$10^3\times10^3$	12.5	3	107.36	87	8.7497×10^{-11}	1.2524×10^{-9}
Deformed	$10^3\times10^3$	6.5	5	6.30	22	5.3848×10^{-11}	3.2586×10^{-10}
Deformed	$10^3\times10^3$	12.5	5	38.73	54	6.4973×10^{-11}	9.4807×10^{-10}

Sections 6.1–6.3 present attractive capabilities of the proposed method. We have applied it on matrices with dimension up to $m = 10^8$ with good results: the error was reduced by at least 10^3. When the technique is used for sampling from a normal distribution of a covariance matrix K, the discrepancy between our simulation and the sought-after distribution is a normal multivariate distribution with at most 10^{-3} relative variance. Moreover, for Gaussian processes with compact kernels, our error estimate indicates that the discrepancy will be much smaller (10^{-9}–10^{-11}). Extrapolation from the 10^4 case and the 10^6 case (Tables 6.2 and 6.3) suggests that an error of 10^{-9} is achievable virtually independent of dimension, by using about $k = 100$ matrix-vector multiplications and thus including the extreme-scale cases that are our ultimate goal.

Of course, for assessing the sought-after 10^{12}–10^{15} range for the number of sites, a parallel program on a high-performance computer will be required. Nevertheless, our approach is factorization-free and thus easily parallelizable. In addition, several efficient ways of estimating the error were given that were demonstrated to be accurate for a large class of matrices. It would be instructive to undertake more extensive computational studies of the relationship between these error estimates and the number k of matrix-vector evaluations.

6.4. Comparison with a related method. In [29], a conjugate residual-type (CR-type) method was proposed which can be adapted for computing $f(A)b = A^{1/2}b$. Instead of computing a polynomial $\phi_{k+1}(t)$ to minimize $\|s(t) - \phi(t)\|$ among all the

polynomials $\phi(t)$ of degree not exceeding k, the CR approach computes a different polynomial $\tilde{\phi}_k(t)$ that minimizes $\left\| s(t) - t\tilde{\phi}(t) \right\|$ among all the polynomials $\tilde{\phi}(t)$ of degree not exceeding $k-1$. In other words, to approximate the spline, the proposed algorithm in this paper uses the polynomial $\phi_{k+1}(t) \in \mathbb{P}_{k+1}$, whereas the CR approach uses $\tilde{\phi}_{k+1}(t) = t\tilde{\phi}_k(t)$, where $\tilde{\phi}_k(t) \in \mathbb{P}_k$. The approximation vector from the CR approach algorithm in [29] is thus $A\tilde{\phi}_k(A)b$. From a conceptual point of view the only difference between the two methods is that the CR approach constrains the sought polynomial to have a value of zero at the origin. From a practical point of view the two approaches differ significantly in their implementation. The CR approach draws a parallel with the solution of linear systems and generates a solution polynomial that can be viewed as a residual polynomial of the form $1 - t\tilde{\phi}(t)$ (which therefore approximates the function $1 - s(t)$). Comparisons between the two approaches were made and will not be reproduced here. In short, the two methods deliver similar results, and this is not too surprising.

Note that in the CR approach the polynomial that approximates the spline, $t\tilde{\phi}_k(t)$, has a zero at the origin so it cannot be directly applied as it can when the function/spline $s(t)$ is nonzero at the origin. However, as was seen above (see also [29]), one can consider the "residual polynomial" $1 - t\tilde{\phi}_k(t)$ as the approximating function $\tilde{\phi}_{k+1}$, since this is known to approximate the function $1 - s(t)$, which now has the value 1 (or indeed any other value by using scaling) at the origin. So, this approach forces the polynomial and the function to have the same value at the origin (or some other point).

6.5. Tests with other functions. We further tested the proposed algorithm on two other functions, the natural logarithm and the exponential, using the same set of matrices in Section 6.1. The logarithm has even larger derivatives than does the square root for t close to the origin; hence it is expected that $\log(A)b$ will be much harder to compute. Since the shapes of log and square root look similar, we used the same interval scheme as for the square root. On the other hand, a trick to handling the exponential is to scale the matrix such that its spectral radius is equal to 1, since the derivative of $\exp(t)$ on the interval $[-1, 1]$ is bounded by a small value e. By performing such a preprocessing, the conditioning of the matrix is no longer a challenge, and therefore it is not necessary to use the same interval scheme as described in Section 5.2 to perform the spline fitting. We simply used $\log(m)$ knots that were evenly distributed on the spectrum of A.

The numerical results are listed in Table 6.4. Compared with Table 6.1, it is clear, and expected, that $\log(A)b$ is harder to approximate than $A^{1/2}b$. A fact not shown in the table is that the approximation quality of $\log(K)b$, for the covariance matrix K of the test of Section 6.3, is appealing: We obtained an error estimate no larger than 10^{-10} for $k = 100$ for both the deformed and undeformed mesh cases. This is expected because these matrices are moderately conditioned. Moreover, the results for $\exp(A)b$ indicate a quality of approximation that does not depend on the condition number of the matrix.

7. Concluding remarks. We have presented a least squares polynomial approximation method for computing a function of a matrix times a vector $f(A)b$. The method first approximates the function $f(t)$ by a spline $s(t)$ and then projects $s(t)$ onto a polynomial subspace such that $s(A)b$ can be (approximately) evaluated as a polynomial of A times b. This technique avoids explicitly forming $f(A)$; and the matrix A is referenced only through k matrix-vector multiplications, where k is the

TABLE 6.4
Numerical results for other functions.

Matrix	κ	$\log(A)b$		$\exp(A)b$	
		k	Residual	k	Residual
Boeing/crystm01	2.2831×10^{2}	54	1.3587×10^{-6}	9	6.5177×10^{-6}
Bates/Chem97ZtZ	2.4721×10^{2}	70	4.0998×10^{-6}	9	9.3029×10^{-6}
JGD/Trefethen_2000	1.5518×10^{4}	200	1.8060×10^{-4}	9	9.2387×10^{-6}
TKK/plbuckle	1.2833×10^{6}	200	1.0433×10^{-2}	9	1.3273×10^{-5}
Nasa/nasa1824	1.8960×10^{6}	200	2.6332×10^{-2}	9	1.2317×10^{-5}
HB/1138_bus	8.5726×10^{6}	200	9.0505×10^{-2}	9	7.0982×10^{-6}
Oberwolfach/t2dal_e	3.7662×10^{7}	200	3.4874×10^{-2}	9	5.3765×10^{-6}
HB/bcsstk12	2.2119×10^{8}	200	5.2497×10^{-2}	9	1.5450×10^{-5}
FIDAP/ex3	1.6838×10^{10}	200	1.5316×10^{-1}	9	7.9267×10^{-6}
Bai/mhd3200b	1.6035×10^{13}	200	1.5902×10^{-1}	11	2.4630×10^{-6}

degree of the polynomial.

The quality of the approximation obtained from the method depends on the nature of the function f. Specific interval schemes for using a spline to fit the function must be defined individually for each f. We discussed the case $f(t) = \sqrt{t}$ in detail and briefly mentioned the case $f(t) = \log(t)$ and $f(t) = \exp(t)$. Analysis shows that in order to yield accurate approximations, it is mandatory to place enough knots on the region where $f'(t)$ is large. By following this guideline, effective interval schemes for other functions can also be derived.

Experiments show that the proposed algorithm is efficient for a practical statistical sampling problem, which involves computing $K^{1/2}b$ for a covariance matrix $K \in \mathbb{R}^{m\times m}$ with a stationary/nonstationary covariance function defined on regular/irregular grids. This application is an example where the matrix A need not be explicitly stored. The algorithm was demonstrated on problems with m up to 10^6, and current results point to promising performance for problems at extreme scales, with $m = 10^{12}$ to 10^{15}.

REFERENCES

[1] E. J. ALLEN, J. BAGLAMA, AND S. K. BOYD, *Numerical approximation of the product of the square root of a matrix with a vector*, Linear Algebra Appl., 310 (2000), pp. 167–181.

[2] Z. BAI, M. FAHEY, AND G. GOLUB, *Some large-scale matrix computation problems*, J. Comput. Appl. Math., 74 (1996), pp. 71–89.

[3] L. BERGAMASCHI, M. CALIARI, AND M. VIANELLO, *Efficient approximation of the exponential operator for discrete 2D advection-diffusion problems*, Numer. Lin. Alg. Appl., 10 (2002), pp. 271–289.

[4] A. CANNING, *Scalable parallel 3D FFTs for electronic structure codes*, in High Performance Computing for Computational Science - VECPAR 2008, Springer, Berlin, 2008, pp. 280–286.

[5] E. CONSTANTINESCU, V. ZAVALA, M. ROCKLIN, S. LEE, AND M. ANITESCU., *Unit commitment with wind power generation: Integrating wind forecast uncertainty and stochastic programming.*, Tech. Memo. ANL/MCS-TM309., Argonne National Laboratory, Mathematics and Computer Science Division, 9700 S Cass Ave, Argonne IL 60439, September 2009. Available online at http://www.mcs.anl.gov/~anitescu/PUBLICATIONS/TM-309.pdf.

[6] P. I. DAVIES AND N. J. HIGHAM, *Computing $f(A)b$ for matrix functions f*, in QCD and Numerical Analysis III, Springer, Berlin, 2005, pp. 15–24.

[7] T. A. DAVIS, *The University of Florida sparse matrix collection*, ACM Trans. Math. Softw., (submitted, 2009).

[8] C. Dietrich and G. Newsam, *Fast and exact simulation of stationary Gaussian processes through circulant embedding of the covariance matrix*, SIAM Journal on Scientific Computing, 18 (1997), pp. 1088–1107.
[9] V. L. Druskin and L. A. Knizhnerman, *Two polynomial methods of calculating functions of symmetric matrices*, USSR Computational Mathematics and Mathematical Physics, 29 (1989), pp. 112–121.
[10] J. Erhel, F. Guyomarc, and Y. Saad, *Least-squares polynomial filters for ill-conditioned linear systems*, Tech. Rep. UMSI 2001/32, University of Minnesota Supercomputing Institute, 2001.
[11] P. Fischer, J. Lottes, D. Pointer, and A. Siegel, *Petascale algorithms for reactor hydrodynamics*, in Journal of Physics: Conference Series, vol. 125(1), Institute of Physics Publishing, 2008, p. 012076.
[12] R. Furrer, M. Genton, and D. Nychka, *Covariance tapering for interpolation of large spatial datasets*, Journal of Computational and Graphical Statistics, 15 (2006), pp. 502–523.
[13] E. Gallopoulos and Y. Saad, *Efficient solution of parabolic equations by Krylov approximation methods*, SIAM J. Sci. and Stat. Comput., 13 (1992), pp. 1236–1264.
[14] G. H. Golub and G. Meurant, *Matrices, moments, and quadrature*, in Numerical Analysis 1993, D. F. Griffiths and G. A. Watson, eds., vol. 303, Pitman, Research Notes in Mathematics, 1994, pp. 105–156.
[15] J. Goodman and A. Sokal, *Multigrid Monte Carlo method: Conceptual foundations.*, Physical Review D: Particles and fields, 40 (1989), p. 2035.
[16] N. J. Higham, *Functions of Matrices: Theory and Computation*, SIAM, 2008.
[17] M. Hochbruck and C. Lubich, *On Krylov subspace approximations to the matrix exponential operator*, SIAM J. Numer. Anal., 34 (1997), pp. 1911–1925.
[18] M. Hochbruck, C. Lubich, and H. Selhofer, *Exponential integrators for large systems of differential equations*, SIAM J. Sci. Comput., 19 (1998), pp. 1552–1574.
[19] C. Kaufman, M. Schervish, and D. Nychka, *Covariance tapering for likelihood-based estimation in large spatial data sets*, Journal of the American Statistical Association, 103 (2008), pp. 1545–1555.
[20] N. N. Lebedev, *Special Functions and Their Applications*, Dover, 1972.
[21] C. Moler and C. Van Loan, *Nineteen dubious ways to compute the exponential of a matrix*, SIAM Review, 20 (1978), pp. 801–836.
[22] ———, *Nineteen dubious ways to compute the exponential of a matrix, twenty-five years later*, SIAM Review, 41 (2003), pp. 3–49.
[23] I. Moret and P. Novati, *The computation of functions of matrices by truncated Faber series*, Numerical Functional Analysis and Optimization, 22 (2001), pp. 697–719.
[24] P. Novati, *A polynomial method based on Fejér points for the computation of functions of unsymmetric matrices*, Applied Numerical Mathematics, 44 (2003), pp. 201–224.
[25] C. Rasmussen and C. Williams, *Gaussian processes for machine learning*, MIT Press, Cambridge, 2006.
[26] T. J. Rivlin, *An Introduction to the Approximation of Functions*, Dover Publications, 1981.
[27] Y. Saad, *Iterative solution of indefinite symmetric systems by methods using orthogonal polynomials over two disjoint intervals*, SIAM J. Numer. Anal., 20 (1983), pp. 784–811.
[28] ———, *Analysis of some Krylov subspace approximations to the matrix exponential operator*, SIAM J. Numer. Anal., 29 (1992), pp. 209–228.
[29] ———, *Filtered conjugate residual-type algorithms with applications*, SIAM J. Matrix Anal. Appl., 28 (2006), pp. 845–870.
[30] K. P. Schmitt, M. Anitescu, and D. Negrut, *Efficient sampling for spatial uncertainty quantification in multibody system dynamics applications*, International Journal for Numerical Methods in Engineering, 80 (2009), pp. 537–564.
[31] M. H. Schultz, *Spline Analysis*, Prentice Hall, 1973.
[32] M. Stein, *Interpolation of Spatial Data: Some theory for Kriging*, Springer-Verlag, Berlin, 1999.
[33] U. Trottenberg, C. Oosterlee, and A. Schuller, *Multigrid*, Academic Press, 2001.
[34] H. A. Van der Vorst, *An iterative solution method for solving $f(A)x = b$, using Krylov subspace information obtained for the symmetric positive definite matrix A*, J. Comput. Appl. Math., 18 (1987), pp. 249–263.
[35] ———, *Solution of $f(A)x = b$ with projection methods for the matrix A*, in Numerical Challenges in Lattice Quantum Chromodynamics, Springer Verlag, Berlin, 2000, pp. 18–28.

The submitted manuscript has been created by the University of Chicago as Operator of Argonne National Laboratory ("Argonne") under Contract No. DE-AC02-06CH11357 with the U.S. Department of Energy. The U.S. Government retains for itself, and others acting on its behalf, a paid-up, nonexclusive, irrevocable worldwide license in said article to reproduce, prepare derivative works, distribute copies to the public, and perform publicly and display publicly, by or on behalf of the Government.